

Dynamics of a solitonic vortex in an anisotropically trapped superfluid

J.M. Gomez Llorente and J. Plata

*Departamento de Física and IUdEA, Universidad de La Laguna,
La Laguna E38200, Tenerife, Spain.*

Abstract

We analytically study the dynamics of a solitonic vortex (SV) in a superfluid confined in a non-axisymmetric harmonic trap. The study provides a framework for analyzing the role of the trap anisotropy in the oscillation of SVs observed in recent experiments on atomic Bose and Fermi superfluids. The emergence of common and statistics-dependent features is traced in a unified approach to both types of fluid. Our description, built in the hydrodynamic formalism, is based on a Lagrangian approach which incorporates the vortex location as dynamical parameters of a variational ansatz. Previous operative Hamiltonian pictures are recovered through a canonically traced procedure. Our results improve the understanding of the experimental findings. Some of the observed features are shown to be specific to the tri-axial anisotropy of the trap. In particular, we characterize the nontrivial dependence of the oscillation frequency on the trapping transversal to the vortical line. The study reveals also the crucial role played by the nonlinear character of the dynamics in the observed oscillation: for the considered experimental conditions, the frequency, and, in turn, the effective inertial mass of the vortex, are found to significantly depend on the amplitude of the generated motion. It is also uncovered how the coupling with collective modes of the fluid induces a non-negligible shift in the oscillation frequency. The appearance of *fine-structure* features in the SV *trajectory* is predicted.

I. INTRODUCTION

The dynamics of solitonic excitations in trapped Bose-Einstein condensates (BECs) have been the subject of intense research in the last decades [1–9]. A central objective of the theoretical work has been the characterization of the effect of trapping on structures identified in uniform environments. Significant advances have been made: different soliton-like solutions, with topological forms depending on the confining characteristics, have been found to the Gross-Pitaevskii (GP) equation. Moreover, the occurrence, dependent on the trapping conditions, in particular, on the effective dimensionality, of dynamical or energetic instability has been traced. Instability-induced decay sequences connecting diverse types of solutions have been described [9–14]. For specific confining properties, planar dark solitons (PDSs), vortex rings (VRs), and SVs are present in a decay cascade initiated via *snake* instability [14–16]. Parallel advances have taken place in the experimental area: various techniques have been implemented for the direct observation and the controlled generation of the structures [1, 2, 5, 6, 8, 17, 18]. The research, initially focused on bosonic fluids, has been extended to superfluid Fermi gases [19–24], where, the distinctive aspects of coherence and interactions imply facing additional, fundamental and technical, problems. In particular, the evaluation of the potential role of the fluid statistics in the appearance of differential characteristics of the soliton-like excitations is required. Here, we deal with some recently uncovered aspects of this problem: experiments realized by different groups have revealed nontrivial features of the dynamics of SVs which seem to be common to fermionic and bosonic superfluids. In those experiments, originally intended to the controlled production of PDSs in a fermionic superfluid in the BEC-BCS crossover [21–23] and in a BEC [18, 25] [26], oscillating long-lived SVs were detected. In fact, the presence of SVs was inferred from the characterization of the observed oscillatory motion, specifically, from tracing unexpected large values of the effective inertial masses. Subsequently, the conclusive identification of the structures as SVs was achieved in the fermionic case through the implementation of direct tomographic imaging. Tomographic techniques also allowed observing instability cascades, where, in agreement with the predictions, PDSs were found to decay into VRs, which, in turn, evolved into SVs [22]. The SV character of the structures was also corroborated in one of the bosonic implementations: observed in free-expansion images, a twisted planar density depletion around the vortex line and phase dislocations in the interference pattern were identified as distinctive

SV signatures [18]. Afterwards, a stroboscopic technique was used to monitor the real-time dynamics [27]. The analyses of the experiments have incorporated numerical simulations based on the GP equation and hydrodynamical approaches [18, 28],[21]. With them, some of the experimental findings have been approximately reproduced. Numerical results were also presented to support the applicability of the technique of control implemented in [26]. Despite those achievements, additional work on the understanding of the experimental results seems necessary. We will focus on three issues that require further clarification. First, an accurate characterization of the role of the trap anisotropy is needed: as emphasized in [26], the lack of models that incorporate the triaxial anisotropy present in some of the practical setups implies that no precise reference values of the oscillation frequencies are available (the associated analyses were based on the approximate applicability of models set up for axisymmetric trapping to the actual anisotropic confinement). Second, removing the limitations of the linear approximation employed in some of the descriptions is essential: the magnitude of the observed amplitudes demands the nonlinear character of the dynamics to be explicitly taken into account. It is worth stressing that, in the nonlinear regime, since the oscillation frequency, and, in turn, the (effective) inertial mass are amplitude dependent, their measured values cannot be identified as intrinsic characteristics of the structures. Third, to achieve a detailed characterization of the system dynamics, some restrictions of the applied formalism must be overcome: although the use of effective Hamiltonian approaches built from approximate expressions for the free energy of the SV has served to understand salient aspects of the dynamics, a more complete description, where second-order effects can be included, is required. To deal with those issues, we generalize the approach presented in [29] to describe the precession of vortex lines in BECs. In this seminal work, the ansatz for the condensate wave function incorporates the phase of a quantum vortex line and the ground-state Thomas-Fermi density. Additionally, the vortex core is modeled by considering a zero-density region around the vortex line with a width given by the healing length. Corrections to such an ansatz will be estimated in the present work. Our results will show the basic approach to be rather accurate. We build a general framework where the evolution of SVs in Bose or Fermi superfluids can be analyzed. Focusing on the dynamics subsequent to the SV formation, we will proceed by setting up a variational scheme where the vortex position will be incorporated as dynamical parameters of the ansatz. In this approach, diverse characteristics of the setups, like different regimes of trap anisotropy or a broad range

of oscillation amplitudes, can be addressed. To account for second-order effects, the trial *wave-function* will be generalized along two lines. First, we will assess the role of additional degrees of freedom of the vortex motion associated to (potentially realizable) sets of initial conditions. Subsequently, the coupling with collective modes of the fluid will be evaluated. The resulting framework will enable us to improve the agreement with the experimental results and predict the appearance of nontrivial *fine-structure* features.

The outline of the paper is as follows. In Sec. II, we present our model system. The variational method used to characterize the dynamics is introduced in Sec. III. As a proof of consistency, we connect with previous operative approaches by presenting a completely traced application of the Hamiltonian formalism. In Sec. IV, the general dynamical equations are particularized to the cases of a BEC and of a superfluid Fermi gas of atoms in the BEC-BCS crossover [30–32]. Additional information on the dynamics, extracted from the generalization of the variational ansatz, is discussed in Sec. V. Some details of the application of our approach to the considered experiments are given in Sec. VI. Finally, the general conclusions are summarized in Sec. VII.

II. THE MODEL SYSTEM

We consider an atomic Bose or Fermi superfluid characterized by an order parameter $\Psi(\mathbf{r}, t) = \sqrt{\rho(\mathbf{r}, t)}e^{iS(\mathbf{r}, t)}$ [$\rho(\mathbf{r}, t)$ and $S(\mathbf{r}, t)$ are respectively the density and phase of the fluid] which is assumed to obey the nonlinear Schrödinger (NLS) equation

$$i\hbar\frac{\partial\Psi(\mathbf{r}, t)}{\partial t} = \left[-\frac{\hbar^2}{2M}\nabla^2 + V_{ex}(\mathbf{r}) + \mu[\rho(\mathbf{r}, t)] \right] \Psi(\mathbf{r}, t). \quad (1)$$

The identification of the parameters in this equation depends on the bosonic or fermionic character of the fluid. For a Bose fluid, M denotes the mass m_A of a condensate atom, and $\mu[\rho(\mathbf{r}, t)]$ accounts for the interaction term, $g\rho$, g being the coupling strength. Eq. (1) corresponds then to the GP equation [30]. On the other hand, for a fermionic fluid in the BEC-BCS crossover, M stands for the mass of a pair of atoms ($M = 2m_A$) and the nonlinear term incorporates the equation of state of the fluid which expresses the chemical potential μ as a function of the density. Moreover, assuming the applicability of the polytropic approximation [33–35], the nonlinear term is written as $\mu[\rho(\mathbf{r}, t)] = C\rho(\mathbf{r}, t)^\gamma$, where the polytropic index γ is a characteristic of the (interaction-dependent) fluid regime, and C is a

constant, which is usually expressed in terms of reference values for the chemical potential and density. In the BEC side of the crossover, the polytropic index takes the value $\gamma = 1$ [Eq. (1) can be again identified with the GP equation]. Additionally, in the unitary regime [21, 31, 32], the dynamics can be expected to be modeled by taking $\gamma = 2/3$. Since no formal differences exist between the description of the bosonic case and that of the fermionic superfluid in the (molecular) BEC regime, we will account for them in a unified way.

Emulating the referred practical setups, a confining nonaxisymmetric harmonic potential $V_{ex}(\mathbf{r})$ is considered, i.e.,

$$V_{ex}(x, y, z) = \frac{1}{2} (k_x x^2 + k_y y^2 + k_z z^2), \quad (2)$$

where k_i ($i \equiv x, y, z$) denote the force constants of the trap, the corresponding frequencies being $\omega_i = \sqrt{\frac{k_i}{m_A}}$. As in the experimental arrangements [21, 26], we consider cigar-shaped traps with transversal anisotropy, specifically, it is assumed that $k_y > k_x \gg k_z$. The SVs were observed to be oriented along the shortest confining direction (OY axis), which was argued to be a consequence of energetic instability. We will tackle this issue farther on. Additionally, we will show that the trap frequencies that directly affect the observed precession frequencies are those transversal to SV orientation, i.e., ω_x and ω_z .

To obtain stationary solutions to Eq. (1), we make the change

$$\Psi(\mathbf{r}, t) = \sqrt{\rho(\mathbf{r})} e^{-\frac{i}{\hbar} \bar{\mu} t}, \quad (3)$$

where $\bar{\mu}$ stands for the effective (bulk) chemical potential. In the resulting (stationary) equation, the Thomas-Fermi (TF) approximation, which corresponds to neglect the kinetic-energy term, implies making

$$V_{ex}(\mathbf{r}) + \mu[\rho(\mathbf{r})] = \bar{\mu}. \quad (4)$$

Then, taking into account the polytropic approximation to $\mu[\rho(\mathbf{r})]$, the stationary fluid density in the TF regime can be written as

$$\begin{aligned} \rho(\mathbf{r}) &= |\Psi(\mathbf{r})|^2 = C^{-1/\gamma} [\bar{\mu} - V_{ex}(\mathbf{r})]^{1/\gamma} \\ &= \rho_0 \left[1 - \frac{V_{ex}(\mathbf{r})}{\bar{\mu}} \right]^{1/\gamma}, \end{aligned} \quad (5)$$

for $\bar{\mu} - V_{ex}(\mathbf{r}) \geq 0$, and, $\rho(\mathbf{r}) = 0$, otherwise. [We have written $\rho(\mathbf{0}) \equiv \rho_0$.] The TF radii R_i , ($i \equiv x, y, z$), are given by

$$R_i = \sqrt{\frac{2\bar{\mu}}{k_i}}, \quad (6)$$

$\bar{\mu}$ being obtained from normalization.

The requirements for the validity of the present approach must be emphasized. First, the hydrodynamic description is expected to be valid at length scales much larger than the healing length. Second, the above NLS equation [Eq. (1)] is applicable provided that a local density approximation to the equation of state of the fluid is feasible. Those conditions are fulfilled in the mentioned experiments.

III. DESCRIPTION OF THE DYNAMICS THROUGH A VARIATIONAL LAGRANGIAN APPROACH

A. General dynamical equations

The NLS equation given by Eq. (1) with $\mu[\rho(\mathbf{r}, t)] = C\rho(\mathbf{r}, t)^\gamma$ can be derived from the Lagrangian density

$$\mathcal{L}[\Psi] = i\frac{\hbar}{2} \left(\Psi^* \frac{\partial \Psi}{\partial t} - \Psi \frac{\partial \Psi^*}{\partial t} \right) - \frac{\hbar^2}{2M} |\nabla \Psi|^2 - V_{ex} |\Psi|^2 - \frac{C}{\gamma+1} |\Psi|^{2(\gamma+1)} \quad (7)$$

Indeed, the NLS equation is the Euler-Lagrange equation that is obtained by imposing the action

$$\mathcal{S}[\Psi] = \int_{t_1}^{t_2} dt \int d\mathbf{r} \mathcal{L}[\Psi] \quad (8)$$

to be stationary against infinitesimal variations $\delta\Psi$ and $\delta\Psi^*$ which fulfill $\delta\Psi(\mathbf{r}, t_1) = \delta\Psi(\mathbf{r}, t_2) = 0, \forall \mathbf{r}$. This Lagrangian formalism provides us with an appropriate framework for setting up a variational method [36]. First, an ansatz $\Psi(\mathbf{r}, t; \mathbf{u})$ is proposed for the *wave function*. (A generic notation, \mathbf{u} , is used for the variational parameters.) Then, by introducing the ansatz into Ec. (7), and integrating, a Lagrangian function is obtained, i.e.,

$$L(\mathbf{u}, \dot{\mathbf{u}}, t) = \int d\mathbf{r} \mathcal{L}[\Psi(\mathbf{r}, t; \mathbf{u}), \Psi^*(\mathbf{r}, t; \mathbf{u})]. \quad (9)$$

Finally, the effective Lagrange's equations

$$\frac{d}{dt} \left(\frac{\partial L}{\partial \dot{\mathbf{u}}} \right) - \frac{\partial L}{\partial \mathbf{u}} = 0, \quad (10)$$

give the dynamics of the variational parameters, and, consequently, the time evolution of $\Psi(\mathbf{r}, t; u)$.

In order to describe the dynamics of the considered solitonic vortex, assumed to be aligned along the y direction, we use the ansatz

$$\Psi(\mathbf{r}, t; x_0, z_0) = |\Psi(\mathbf{r})| e^{iS(x, z; t; x_0, z_0)}, \quad (11)$$

where the variational parameters, x_0 , and z_0 , correspond to the time-dependent location $\mathbf{r}_0(t) = [x_0(t), z_0(t)]$ of the SV which we intend to characterize. For the phase profile, which must account for the circulating flow around the vortex, we write

$$\begin{aligned} S(x, z, t; x_0, z_0) &= \arctan \left(\frac{x - x_0}{z - z_0} \right) - \frac{\bar{\mu}t}{\hbar} \\ &\equiv S_v(x, z; x_0, z_0) - \frac{\bar{\mu}t}{\hbar}. \end{aligned} \quad (12)$$

Additionally, for $|\Psi(\mathbf{r})|$, we take the background Thomas-Fermi (TF) expression, given through Ec. (5): as a first-order approximation, it is assumed here that the modification of the background density due to the presence of the vortex has a minor effect on the characterization of the parameter dynamics. Second-order effects will be evaluated in Section V, where we will use a more elaborate ansatz which incorporates changes in the density correlated with the phase proposal and accounts for the potential interplay of the vortex motion with collective modes of the fluid. These changes will also allow a more precise evaluation of the effects of the vortex core.

The dynamics of the parameters x_0 and z_0 are governed by the Lagrangian function obtained from Eq. (9), i.e.,

$$L(x_0, z_0; \dot{x}_0, \dot{z}_0) = \int d\mathbf{r} \left[-\hbar\rho \frac{\partial(S_v - \frac{\bar{\mu}t}{\hbar})}{\partial t} - \frac{\hbar^2}{2M} (|\nabla\rho^{1/2}|^2 + \rho|\nabla S|^2) - V_{ex}\rho - \frac{C\rho^{\gamma+1}}{\gamma+1} \right] \quad (13)$$

where we have taken into account that

$$i\frac{\hbar}{2} \left(\Psi^* \frac{\partial\Psi}{\partial t} - \Psi \frac{\partial\Psi^*}{\partial t} \right) = -\hbar\rho \frac{\partial S}{\partial t}, \quad (14)$$

and,

$$|\nabla\Psi|^2 = |\nabla\rho^{1/2} + i\rho^{1/2}\nabla S|^2. \quad (15)$$

Given the form of the ansatz [see Eq. (11)] which incorporates the variational parameters only through the phase $S_v(x, z; x_0, z_0)$, it is apparent that the terms associated with $\bar{\mu}$, $|\nabla\rho^{1/2}|^2$, $V_{ex}\rho$, and $\frac{C}{\gamma+1}\rho^{\gamma+1}$ in Eq. (13) are not relevant to the effective Lagrange's equations as they do not introduce dependence on the parameters. (Furthermore, since the term $|\nabla\rho^{1/2}|^2$ is neglected in the considered TF approximation, it will yet be ignored in the forthcoming generalization of the ansatz, in spite of the parameters being incorporated then, not only through the phase, but also via the density.) Hence, the Lagrangian function can be effectively reduced to

$$L(x_0, z_0; \dot{x}_0, \dot{z}_0) = \int d\mathbf{r}\rho \left[-\hbar\frac{\partial S_v}{\partial t} - \frac{\hbar^2}{2M} |\nabla S_v|^2 \right]. \quad (16)$$

The integration must exclude the region around the solitonic-vortex core (a cylinder of radius equal to the healing length) where the true condensate density can be accurately approximated to zero. This approximation, which has been used, in all theoretical previous works of confined vortex lines, regularizes the integral. Using the specific functional form proposed for the phase in Eq. (12), we rewrite Eq. (16) as

$$\begin{aligned} L(x_0, z_0; \dot{x}_0, \dot{z}_0) &= \int d\mathbf{r}\rho(\mathbf{r}) \frac{\hbar [\dot{x}_0(z - z_0) - \dot{z}_0(x - x_0)] - \frac{\hbar^2}{2M}}{(x - x_0)^2 + (z - z_0)^2} \\ &\equiv f_x(x_0, z_0)\dot{x}_0 + f_z(x_0, z_0)\dot{z}_0 + F(x_0, z_0), \end{aligned} \quad (17)$$

where, for convenience for the later application of the Hamiltonian formalism, we have introduced the functions

$$f_x(x_0, z_0) = \hbar \int d\mathbf{r}\rho(\mathbf{r}) \frac{(z - z_0)}{(x - x_0)^2 + (z - z_0)^2}, \quad (18)$$

$$f_z(x_0, z_0) = -\hbar \int d\mathbf{r}\rho(\mathbf{r}) \frac{(x - x_0)}{(x - x_0)^2 + (z - z_0)^2}, \quad (19)$$

$$F(x_0, z_0) = -\frac{\hbar^2}{2M} \int d\mathbf{r}\rho(\mathbf{r}) \frac{1}{(x - x_0)^2 + (z - z_0)^2}, \quad (20)$$

which have been evaluated using an approximate method of sequential integration applicable in the regime of strong anisotropy corresponding to the referred experiments, i.e., for $\omega_x \gg$

ω_z . Here, we recall that, in the realization of [21], which corresponded to a fermionic superfluid in the BEC-BCS crossover, the displacement of the center of the (cigar-shaped) trap due to gravitational effects led to a small difference between the values of the trap frequencies in the directions perpendicular to the longest trap axis. Consequently, the system was not axially symmetric, the anisotropy transversal to the vortical line being considerable. Also, the trap used in the experimental realization corresponding to an atomic BEC [26] was operated in a regime of strong anisotropy. We have obtained for the above integrals

$$f_x(x_0, z_0) \simeq 0, \quad (21)$$

$$f_z(x_0, z_0) \simeq -\pi\hbar \int_{-x_0}^{x_0} \rho_{2D}(x, z_0) dx, \quad (22)$$

$$F(x_0, z_0) \simeq -\frac{\pi\hbar^2}{M} \rho_{2D}(x_0, z_0) \ln\left(\frac{R_x}{\xi}\right). \quad (23)$$

where R_x is the TF radius in the x direction [see Eq. (6)] and ξ represents the size of the vortex core, which, for, both, bosonic and fermionic fluids, can be approximated as $\xi = \hbar/\sqrt{2M\bar{\mu}}$ within the TF picture. Note that ξ corresponds to the standard form of the healing length in the bosonic case. Moreover, we have used the column density along the vortex orientation, i.e.,

$$\rho_{2D}(x, z) = \int_{-y_L(x,z)}^{y_L(x,z)} \rho(x, y, z) dy. \quad (24)$$

where,

$$y_L(x, z) = +\frac{1}{k_y^{1/2}} [2\bar{\mu} - (k_x x^2 + k_z z^2)]^{1/2} \quad (25)$$

is the limit value of the y -coordinate as a function of the other two variables. We have employed (alternative) methods of integration of general applicability to precisely define the range of validity of the obtained Lagrangian function. Namely, although exact values of the integrals present in Eqs. (18) and (19) have not been explicitly obtained, they can be shown to lead to the same Lagrangian function as the expressions given by Eqs. (21) and (22). Then, it follows that the approximation implemented to obtain $f_x(x_0, z_0)$ and $f_z(x_0, z_0)$ does not restrict the applicability of the description. Additionally, in order to improve the accuracy of Eq. (23), we have gone to the next precision order: we have calculated the contribution of the zero-order terms (i.e, the terms where the factor R_x/ξ is not present). That contribution will be incorporated through a numerical factor, the *effective zero-order parameter* $c_\gamma^{(0)}$, in

the argument of the logarithmic function in Eq. (23), namely, we will write $\ln(c_\gamma^{(0)} R_x/\xi)$. In Sec. V, we will see that the generalization of the description implies dealing with additional zero-order terms, which will be accounted for by appropriately modifying $c_\gamma^{(0)}$. The final value of that parameter, which entirely incorporates the zero-order terms of the different extensions of the model, will be given in Sec. VI, when the specific application of the study to the experimental setups is discussed.

Using the explicit forms of $f_x(x_0, z_0)$, $f_z(x_0, z_0)$, and $F(x_0, z_0)$, the Lagrangian function is written as

$$L(x_0, z_0; \dot{x}_0, \dot{z}_0) = -\pi\hbar\dot{z}_0 \int_{-x_0}^{x_0} \rho_{2D}(x, z_0) dx - \pi \frac{\hbar^2}{M} \rho_{2D}(x_0, z_0) \ln \left(c_\gamma^{(0)} \frac{R_x}{\xi} \right), \quad (26)$$

and, from Lagrange's equations, one obtains that the evolution of the vortex location is given by

$$\dot{x}_0 = \frac{\hbar}{2M} \frac{\frac{\partial \rho_{2D}(x_0, z_0)}{\partial z_0}}{\rho_{2D}(x_0, z_0)} \ln \left(c_\gamma^{(0)} \frac{R_x}{\xi} \right) \quad (27)$$

$$\dot{z}_0 = -\frac{\hbar}{2M} \frac{\frac{\partial \rho_{2D}(x_0, z_0)}{\partial x_0}}{\rho_{2D}(x_0, z_0)} \ln \left(c_\gamma^{(0)} \frac{R_x}{\xi} \right). \quad (28)$$

Here, it is apparent that much of the information on the dynamics is incorporated into the column density. It is via $\rho_{2D}(x_0, z_0)$ that the anisotropy of the trap and the nonlinearity of the problem enter the equations. Moreover, in the present approach, the differences between the dynamics of the SV in bosonic and fermionic superfluids emerge mainly from the different form of the column density in each case. Later on, the specific functional form of $\rho_{2D}(x_0, z_0)$ will be introduced and the characteristic frequency of the oscillation Ω_p will be obtained. We will see that the presence of the quotient $(\partial \rho_{2D}/\partial z_0)/\rho_{2D}$ [or $(\partial \rho_{2D}/\partial x_0)/\rho_{2D}$] in the above equations implies that Ω_p does not explicitly depend on the trap frequency along the SV direction ω_y .

Some considerations on dimensionality are pertinent. The dynamical system formed by the set of variational parameters has only one degree of freedom: since the Lagrangian presents a linear dependence on the generalized velocities, the dynamics are given by two first-order equations. In consequence, only two initial conditions, e.g., the vortex coordinates $x_0(t=0)$, $z_0(t=0)$, are required. Note that the dimensionality constraints derive from the form chosen for the variational ansatz. A reduction in the set of generalized coordinates will be implemented in the next subsection.

B. The Hamiltonian formalism

An operative Hamiltonian picture set up from an approximate expression for the free energy of the SV was presented in [21] and subsequently used in [11]. (The same technique had been applied to analyze the dynamics of a vortex ring in [37]; see also [38, 39] for alternative approaches.) To establish the connection with those descriptions, we give now a detailed account of the application of the Hamiltonian formalism to our model system.

Since building the Hamiltonian function from a redundant set of generalized coordinates can lead to inconsistencies, we turn to implement a dimensionality reduction, prior to the derivation of Hamilton equations. In order to present a general procedure, explicit expressions for the functions $f_x(x_0, z_0)$, $f_z(x_0, z_0)$, and $F(x_0, z_0)$ will not be used. We start by rewriting the Lagrangian function that governs the dynamics: to the expression of $L(x_0, z_0; \dot{x}_0, \dot{z}_0)$ given by Ec. (17), we add the total time derivative of a function $G(x_0, z_0)$, which will be adjusted in order to eliminate one of the generalized velocities. (Without loss of generality we will remove \dot{x}_0 .) Hence, the *new* Lagrangian function is written as

$$\begin{aligned} \tilde{L}(x_0, z_0; \dot{x}_0, \dot{z}_0) &= f_x(x_0, z_0)\dot{x}_0 + f_z(x_0, z_0)\dot{z}_0 + F(x_0, z_0) + \frac{d}{dt}G(x_0, z_0) \\ &= f_x(x_0, z_0)\dot{x}_0 + f_z(x_0, z_0)\dot{z}_0 + F(x_0, z_0) + \frac{\partial G}{\partial x_0}\dot{x}_0 + \frac{\partial G}{\partial z_0}\dot{z}_0, \end{aligned} \quad (29)$$

and, to eliminate \dot{x}_0 , we impose

$$\frac{\partial G}{\partial x_0} = -f_x(x_0, z_0) \quad (30)$$

Then, $G(x_0, z_0)$ is obtained as

$$G(x_0, z_0) = - \int f_x(x_0, z_0) dx_0, \quad (31)$$

and the Lagrangian function is converted into

$$\tilde{L}(x_0, z_0; \dot{z}_0) = \left[f_z(x_0, z_0) + \frac{\partial G}{\partial z_0} \right] \dot{z}_0 + F(x_0, z_0).$$

It follows that the canonical conjugate momentum of z_0 is given by

$$p_{z_0} = \frac{\partial \tilde{L}}{\partial \dot{z}_0} = f_z(x_0, z_0) + \frac{\partial G}{\partial z_0}, \quad (32)$$

and the Hamiltonian function is straightforwardly set up through a Legendre transformation. Namely,

$$H(z_0, p_{z_0}) = p_{z_0} \dot{z}_0 - \tilde{L} = -F[z_0, x_0(z_0, p_{z_0})] \quad (33)$$

[We have written $x_0(z_0, p_{z_0})$ from Ec. (32): there are only two canonical conjugate variables, z_0 and p_{z_0} .] The expression obtained for $H(z_0, p_{z_0})$, particularized to the axis-symmetric scenario, matches the effective Hamiltonian function operatively built from the free energy in previous approaches [21] [11]. Actually, in those descriptions, the energy was evaluated from modeling the SV *wave-function* in a form analogous to the ansatz proposed in our variational method. No *ad hoc* introduction of the conjugate momentum is required in our approach: a completely canonical procedure is followed.

Hamilton's equations are given by the expressions

$$\dot{z}_0 = \frac{\partial H}{\partial p_{z_0}} = -\frac{\partial F}{\partial x_0} \frac{\partial x_0}{\partial p_{z_0}}, \quad (34)$$

$$\dot{p}_{z_0} = -\frac{\partial H}{\partial z_0} = \left[\frac{\partial F}{\partial z_0} \right]_{x_0} + \frac{\partial F}{\partial x_0} \frac{\partial x_0}{\partial z_0}, \quad (35)$$

which, after minor algebra, are shown to consistently reproduce the dynamical equations obtained via the Lagrangian formalism [Ecs. (27) and (28)]. This alternative view of the evolution of the parameters can be convenient for further studies where analogies with other dynamical systems can be established via canonical transformations.

At this point it is worth recalling that, in the referred experiments [26], [21], the SVs were found to be oriented along the shortest axis of the trap. Some insight into this finding can be achieved by analyzing the expression of the Hamiltonian [Ec. (33)] for a generic orientation of the vortex. It is shown that the lowest energy of the system corresponds indeed to the vortical line oriented along the shortest radius. Consequently, one can conjecture that there must be a damping mechanism which leads to the occurrence of that minimum-energy orientation. (Dissipation effects on related structures were studied in [40–44].) Closely connected with this aspect of the dynamics is the characterization of the initial conditions for the analyzed process. In fact, this is an open question: the possibility of preparing the initial state is limited as the SVs seem to appear as the (uncontrolled) final product of decay sequences which start with PDSs. Further restrictions on the initial conditions are present

if, as conjectured, the SVs experience a damping process leading to the minimum-energy orientation. Actually, from the potential effects of decay and damping, one can reasonably expect the emergence of a constrained scenario for the effective preparation of the SVs. The pertinence of a simple set of two initial conditions, e.g., the coordinates of the vortical line, as required in the above approach, seems to be corroborated by the general agreement of our basic picture with the experimental results. On the other hand, a potential realization where both, the initial positions and velocities of the structures, could be independently fixed would require an approach with a more elaborate ansatz where the dimensional reduction outlined in the above paragraphs would not be feasible. We will deal with this issue in Sec. V.

IV. THE ROLE OF THE FLUID STATISTICS IN THE VORTEX DYNAMICS

In our picture, the differential characteristics of the SV dynamics in bosonic and fermionic superfluids are rooted in the corresponding different values of the polytropic index of the applied NLS equation. Furthermore, given the form of the ansatz used in the variational method, γ enters the description through the background density $\rho(\mathbf{r})$, more specifically, via the column density $\rho_{2D}(x, z)$ and the effective factor $c_\gamma^{(0)}$ in Eqs. (27) and (28). To make explicit the differences between the bosonic and fermionic cases, we evaluate the precise functional form of that density: using the scaled variables

$$X = \frac{x}{R_x}, \quad Y = \frac{y}{R_y}, \quad Z = \frac{z}{R_z}, \quad (36)$$

the expression of the TF density in the bosonic case (i.e., for, both, bosonic atoms and fermionic atoms in the BEC regime) is written as

$$\rho_B(X, Y, Z) = \rho_0 (1 - X^2 - Y^2 - Z^2). \quad (37)$$

On the other hand, in the fermionic case at the unitarity regime, the TF density reads

$$\rho_F(X, Y, Z) = \rho_0 (1 - X^2 - Y^2 - Z^2)^{3/2}. \quad (38)$$

Both expressions are applicable in the range defined by $1 \geq X^2 + Y^2 + Z^2$, the density being zero outside that range. The respective column densities, $\rho_{2D,B}(X, Z)$ and $\rho_{2D,F}(X, Z)$, are in turn given by

$$\rho_{2D,B}(X, Z) = \frac{4}{3} R_y \rho_0 (1 - X^2 - Z^2)^{3/2}, \quad (39)$$

and

$$\rho_{2D,F}(X, Z) = \frac{3}{8} \pi R_y \rho_0 (1 - X^2 - Z^2)^2. \quad (40)$$

Introducing those expressions into Ecs. (27) and (28), we obtain the evolution of the vortex location, which can be expressed in compact form, for both $\gamma = 1$ and $\gamma = 2/3$, as

$$\dot{X}_0 = -\frac{2\gamma^{-1} + 1}{4} \frac{\hbar \sqrt{k_x k_z}}{\bar{\mu} M} \ln \left(c_\gamma^{(0)} \frac{R_x}{\xi} \right) \frac{Z_0}{1 - X_0^2 - Z_0^2} \quad (41)$$

$$\dot{Z}_0 = \frac{2\gamma^{-1} + 1}{4} \frac{\hbar \sqrt{k_x k_z}}{\bar{\mu} M} \ln \left(c_\gamma^{(0)} \frac{R_x}{\xi} \right) \frac{X_0}{1 - X_0^2 - Z_0^2} \quad (42)$$

From these equations, it is readily shown that the amplitude of the SV motion, given by

$$A_{xz} = \sqrt{X_0^2 + Z_0^2}, \quad (43)$$

is a conserved magnitude satisfying $0 \leq A_{xz} \leq 1$. Indeed, the vortex location describes the elliptical trajectory defined by the equation

$$\frac{x_0^2}{R_x^2} + \frac{z_0^2}{R_z^2} = A_{xz}^2, \quad (44)$$

which actually corresponds to the most conspicuous experimental features. (Perturbative corrections to this description, which will be presented in the next section, will allow us to predict the emergence of fine-structure characteristics.) Moreover, we can combine Eqs. (41) and (42), to obtain

$$\ddot{X}_0 + \Omega_p^2 X_0 = 0, \quad (45)$$

and

$$\ddot{Z}_0 + \Omega_p^2 Z_0 = 0, \quad (46)$$

where the characteristic frequency of the vortex oscillation is

$$\Omega_p = \frac{2\gamma^{-1} + 1}{4} \frac{\hbar \sqrt{k_x k_z}}{\bar{\mu} M (1 - A_{xz}^2)} \ln \left(c_\gamma^{(0)} \frac{R_x}{\xi} \right). \quad (47)$$

In order to compare with the experimental results, it is convenient to express Ω_p as a function of the trap frequencies $\omega_i = \sqrt{\frac{k_i}{m_A}}$, ($i \equiv x, y, z$). For a Bose gas of atoms, since $M = m_A$ and $\gamma = 1$, we find

$$\Omega_{p,B} = \frac{3\hbar}{4\bar{\mu}} \frac{\omega_x \omega_z}{(1 - A_{xz}^2)} \ln \left(c_{\gamma=1}^{(0)} \frac{R_x}{\xi} \right). \quad (48)$$

In contrast, for a Fermi superfluid, taking into account that $M = 2m_A$, one obtains

$$\Omega_{p,F} = \frac{2\gamma^{-1} + 1}{8} \frac{\hbar}{\bar{\mu}} \frac{\omega_x \omega_z}{(1 - A_{xz}^2)} \ln \left(c_{\gamma}^{(0)} \frac{R_x}{\xi} \right). \quad (49)$$

Some preliminary clues to clarify the experimental findings can be extracted from the above picture:

i) The lack of models strictly applicable to a triaxial anisotropic confinement was a handicap in the early interpretation of the experimental results. In fact, former analyses were based on assuming the approximate applicability of theoretical results known for an axisymmetric trapping. From the initial interpretation of the findings as reflecting the effect of the transversal trapping on the reduced mono-dimensional motion of the observed structure, the oscillation frequency was conjectured to depend on the trap frequencies transversal to the longest radius of the (cigar-shaped) trap. In order to reproduce the observed features, an effective mean value of the two transversal frequencies, tentatively defined in different forms, was used in the expression known for the axisymmetric setting [26]. Moreover, an effective transversal radius R_t was incorporated in the logarithmic factor present in the functional form of the frequency, i.e., $\ln(R_t/\xi)$. Those limitations of the analysis are removed by the present study. Our results conclusively show that it is the trap anisotropy transversal to the vortex line that affects the precession frequency: as shown in Eqs. (48) and (49), Ω_p depends on both ω_x and ω_z . Moreover, as we have previously stated, Ω_p does not explicitly depend on the trap frequency corresponding to the direction of the vortical line: ω_y enters Eqs. (48) and (49) only through the bulk chemical potential. Our study lifts also the ambiguity relative to the argument of the logarithmic function: it is the radius R_x corresponding to the shortest transversal direction to the vortex line that enters that argument.

ii) Because of the nonlinear character of the dynamics, the oscillation frequency depends on the amplitude A_{xz} . In fact, for the amplitudes detected in the experiments, a linear approximation, i.e., taking $1 - A_{xz}^2 = 1 - X_0^2 - Z_0^2 \simeq 1$, is not feasible, and the specific value

of the factor $1 - A_{xz}^2$ must be taken into account to reproduce the measured frequencies.

A comment on the use of an effective inertial mass in the present context is in order. The introduction of that concept in the study of planar solitons [45] allowed deriving a compact expression for the period of the soliton in terms of the period of the (elongated) trap. In the considered regime of small-amplitude oscillations, the inertial mass is an intrinsic characteristic of the (trapped) solitonic structure. However, in its application to the (two-dimensional) dynamics of the SV made in [21], the inertial mass becomes dependent on the vortex position via the column density. The present analysis shows that there is an additional dependence on the SV position associated to the nonlinearity of the dynamics.

iii) No qualitative differences in the SV dynamics for the bosonic and fermionic cases are predicted with the used variational framework. The only differential effect is a numerical factor determined by the value of the polytropic index γ in the characteristic frequency of oscillation Ω_p and the logarithmic factor c . The common global properties simply derive from the assumed superfluid character of both Bose and Fermi gases.

V. GENERALIZATION OF THE APPROACH

In this Section, the above description will be generalized by increasing the flexibility of the variational ansatz. Two lines will be followed. First, we will use a trial *wave-function* where the vortex-location parameters will be incorporated, not only through the phase, as in the previous approach, but also via the functional form of the density. This will be shown to imply dealing with additional degrees of freedom in the characterization of the vortex dynamics. In the second line, an ansatz which can account for the role of the condensate degrees of freedom will be employed. Although both extensions can be studied simultaneously, we will deal with them consecutively in order to concentrate on their differential implications. For simplicity, only the analysis of SV dynamics in the bosonic superfluid will be presented. For the fermionic case, which can be straightforwardly studied following the same procedure, only the final results will be given.

A. Effects associated to vortex-induced variations in the fluid density

Here, we use the connection between phase and density given by the Euler-like equation of the hydrodynamic formalism [30] to derive the functional form of the density from the form proposed for the phase. Specifically, in the trial *wave-function*, written now as $\Psi = \tilde{\rho}^{1/2} e^{iS}$, our proposal for the phase is

$$S(\mathbf{r}, t; x_0, z_0) = S_v(x, z; x_0, z_0) - \frac{1}{\hbar} \bar{\mu} t + \delta, \quad (50)$$

which still incorporates the *vorticity-conveying* function $S_v(x, z; x_0, z_0)$, given by Eq. (12), and the term associated to the bulk chemical potential $\bar{\mu}$. So there are no differences with the previous proposal except for the presence of the additional parameter $\delta(t)$, needed now to guarantee the normalization of the trial *wave-function* as modifications in the density are introduced. Indeed, the form of the density, $\tilde{\rho}$, is not longer assumed to be that of the background $\rho(\mathbf{r}) = g^{-1} [\bar{\mu} - V_{ex}(\mathbf{r})]$. Now, $\tilde{\rho}$ is left as a free field in the Lagrangian density, it being subsequently fixed by its own Euler-Lagrange equation of motion. It amounts to use the precise connection between density and phase given by the Euler-like (hydrodynamic) equation, i.e.,

$$\frac{\hbar^2}{2M} |\nabla S|^2 + V_{ex} + \hbar \frac{\partial(S_v - \frac{\bar{\mu}t}{\hbar} + \delta)}{\partial t} + g\tilde{\rho} = 0. \quad (51)$$

Accordingly, the density is obtained in terms of the phase as

$$\begin{aligned} \tilde{\rho} &= -\frac{1}{g} \left[\frac{\hbar^2}{2M} |\nabla S|^2 + V_{ex} + \hbar \frac{\partial S_v}{\partial t} - \bar{\mu} + \hbar \dot{\delta} \right] \\ &= \rho - \frac{1}{g} \left[\frac{\hbar^2}{2M} |\nabla S|^2 + \hbar \frac{\partial S_v}{\partial t} + \hbar \dot{\delta} \right]. \end{aligned} \quad (52)$$

This expression is incorporated now into our variational scheme. To derive the Lagrangian function, we first introduce into Eq. (13) the form of the nonlinear term corresponding to the considered bosonic case. It is worth emphasizing that a more complete characterization of the vortex core is given in this approach: the kinetic term, $\frac{\hbar^2}{2M} |\nabla S|^2$, explicitly accounts for the density reduction in the core. The size of the zero-density region is found to correspond to the healing length, as was assumed in the previous simpler model. Actually, the predictions of the present approach confirms the applicability of the basic model as a first-order approximation.

Then, using the link between phase and density given by Eq. (51), the Lagrangian function is written in the compact form

$$L(x_0, z_0; \dot{x}_0, \dot{z}_0) = \frac{g}{2} \int d\mathbf{r} \tilde{\rho}^2. \quad (53)$$

Finally, by inserting in this equation the density as given by Eq. (52), and retaining only the dominant terms, we arrive at

$$\begin{aligned} L(x_0, z_0; \dot{x}_0, \dot{z}_0) = & \frac{g}{2} \int d\mathbf{r} \rho^2 + \\ & \int d\mathbf{r} \rho \left[-\hbar \frac{\partial S_v}{\partial t} - \frac{\hbar^2}{2M} |\nabla S_v|^2 \right] + \\ & \frac{1}{2g} \int d\mathbf{r} \left(\hbar \frac{\partial S_v}{\partial t} \right)^2 + \\ & \frac{1}{2g} \int d\mathbf{r} \left(\frac{\hbar^2}{2M} |\nabla S|^2 \right)^2 \end{aligned} \quad (54)$$

The magnitude of the terms left out in the above equation can be shown to be much smaller than that of the ones kept. We have also omitted the part that accounts for the dynamics of $\delta(t)$, which is uncoupled from the rest of parameters and it is trivially solved in the regime which will be eventually considered. The term $\frac{g}{2} \int d\mathbf{r} \rho^2$ in the above equation can be ignored as it does not contain the variational parameters. The rest of the integrals are evaluated to logarithmic accuracy, including zero-order terms, to give

$$\begin{aligned} L(x_0, z_0; \dot{x}_0, \dot{z}_0) = & -\pi \hbar \dot{z}_0 \int_{-x_0}^{x_0} \rho_{2D}(x, z_0) dx - \pi \frac{\hbar^2}{M} \rho_{2D}(x_0, z_0) \ln \left(c_{\gamma=1}^{(1)} \frac{R_x}{\xi} \right) + \\ & \pi \frac{\hbar^2}{g} \sqrt{\frac{2\bar{\mu}}{M\omega_y^2}} \ln \left(c_{\gamma=1}^{(2)} \frac{R_x}{\xi} \right) (\dot{x}_0^2 + \dot{z}_0^2). \end{aligned} \quad (55)$$

The first line contains the Lagrangian function used in the former approximation. Specific to the modification of the ansatz is the change in the effective zero-order parameter, i.e., $c_{\gamma=1}^{(0)} \rightarrow c_{\gamma=1}^{(1)}$, which is made to account for the contribution of the last integral in Eq. (54), entirely given by zero-order terms. Also emergent is the quadratic function of the generalized velocities present in the second line. (The parameter $c_{\gamma=1}^{(2)}$ is required there.) The magnitude of the changes, which can be approximately evaluated using the dynamical equations of the previous order of approximation, i.e., Eqs. (41) and (42), is shown to be much

smaller than that of the former Lagrangian. As a consequence, the effects incorporated by the implemented modification of the trial *wave-function* can be estimated to correspond to a perturbation of the formerly characterized scenario. Particularly relevant to the consistency of the description is the explicit inclusion of the vortex core in the ansatz used in the modified scenario. The minor effect of this correction justifies the approach followed in previous theoretical works. Namely, the use of an ansatz where the vortex core is modeled by an exclusion region in the background Thomas-Fermi density with size determined by the healing length correctly accounts for the most conspicuous experimental features.

Some more specific conclusions follow:

i) Since the Lagrangian presents a quadratic dependence on the generalized velocities, the dynamics are described now in terms of two second-order equations. Hence, no dimensional reduction can be implemented: both, the initial positions and velocities, are needed to integrate the equations. This approach can then be relevant to potential experimental arrangements where the independent variation of that set of initial conditions could be feasible.

ii) As can be shown from the dynamical equations, the amplitude $A_{xz} = \sqrt{X_0^2 + Z_0^2}$ is not longer a conserved magnitude. Indeed, the amplitude is found to oscillate: Fig. 1 illustrates how the elliptic trajectories of the vortex location found in the previous approach are now modulated by a term oscillating with a frequency larger than the precession frequency.

iii) Useful insight into the mechanisms responsible for the dynamics is given by a linear approximation. One of the normal modes can be basically traced to a linearized version of the model system of the previous order of approximation. Its frequency, i.e., the (linear) counterpart of the precession frequency formerly obtained, is approximately given by

$$\Omega_{p,B} = \frac{3 \hbar \sqrt{k_x k_z}}{4 \bar{\mu} M} \ln \left(c_{\gamma=1}^{(1)} \frac{R_x}{\xi} \right), \quad (56)$$

and

$$\Omega_{p,F} = \frac{\hbar \sqrt{k_x k_z}}{\bar{\mu} M} \ln \left(c_{\gamma=2/3}^{(1)} \frac{R_x}{\xi} \right), \quad (57)$$

for the respective bosonic and fermionic cases. The other mode, which we term *the modulation mode*, is specific to the elements incorporated via variations in the density. Its frequency Ω_m , which is higher than the precession frequency Ω_p , has been obtained through an ana-

lytical adiabatic approximation. Specifically, we have found for Ω_m the following (bosonic and fermionic) expressions

$$\Omega_{m,B} = \frac{8\mu}{3\hbar} \left(\left[2 \ln \left(4 \frac{R_x}{\xi} \right) - 3 \right] \left[2 \ln \left(4 \frac{R_x}{\xi} \right) - 1 - 4 \sqrt{\frac{k_z}{k_x}} \right] \right)^{-1/2} \quad (58)$$

and

$$\Omega_{m,F} = 2 \frac{\mu}{\hbar} \left(\left[2 \ln \left(2 \frac{R_x}{\xi} \right) - 2 \right] \left[2 \ln \left(2 \frac{R_x}{\xi} \right) - 4 \sqrt{\frac{k_z}{k_x}} \right] \right)^{-1/2}, \quad (59)$$

whose validity has been checked through numerical calculations. For generic initial conditions, the global dynamics can be viewed as corresponding to a combination of the two (component) modes of the system. The results of the former description are recovered provided that the initial conditions fulfill Ecs. (41) and (42): only the precession mode is generated then.

iv) The present extension of the approach can be actually regarded as a proof of consistency. The pertinence of improving the primary ansatz by modifying the form of the density according to the precise constraints imposed by the hydrodynamic formalism is clear. Since the former order of approximation has been shown to account for salient features of the dynamics, its robustness against a consistent modification of the ansatz can be expected. The second-order character of the obtained corrections confirms that argument. Following the same line of reasoning, the physical character of the found second-order effects can be presumed. However, their detection implies dealing with technical difficulties: the observation of the additional (larger) frequency Ω_m requires higher experimental resolution. One cannot disregard that the (uncontrolled) conditions for the emergence of the SVs structures might correspond to the inhibition of the second mode. Moreover, we should take into account that the potential resonance of that mode with high-frequency collective excitations of the condensate could activate a damping mechanism which can preclude its observation. The analysis of the robustness of the second mode against dissipation effects is left for future work.

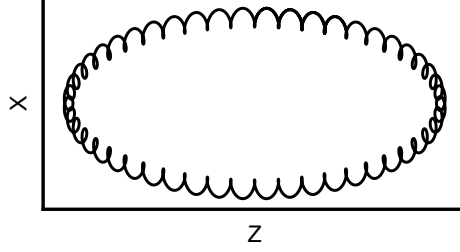


Figure 1: An illustration of a SV trajectory as predicted by the first extension of our basic approach. A perturbative high-frequency modulation of the formerly obtained elliptical trajectory is observed.

B. The effect of the condensate motion on the SV dynamics

Now, we turn to analyze how the characterization of the vortex precession is modified when degrees of freedom of the background fluid are taken into account. The general procedure is illustrated by incorporating the dipole and quadrupole modes into the description. Appropriate to our objectives is the use of a variational ansatz $\Psi = \tilde{\rho}^{1/2} e^{iS}$ with the phase being given by

$$S(\mathbf{r}, t; x_0, z_0; a_j, b_{jk}) = S_v(x, z; x_0, z_0) - \frac{1}{\hbar} \bar{\mu} t + \delta + \sum_{j,k=x,z} a_j x_j + b_{jk} x_j x_k, \quad (60)$$

where, in addition to the vortex location and the normalization term $\delta(t)$, we have included the set of parameters $a_j(t)$ and $b_{jk}(t)$, which will allow dealing with the dipole and quadrupole modes of the fluid. (Only the modes contained in the plane perpendicular to the SV are considered.) Apart from entering the phase, those parameters are present in the form of the density $\tilde{\rho}$, which is derived, as indicated in the previous subsection, through the Euler-like (hydrodynamic) equation that connects phase and density. Accordingly, we obtain

$$\begin{aligned} \tilde{\rho} &= -\frac{1}{g} \left[\frac{\hbar^2}{2M} |\nabla S|^2 + V_{ex} + \hbar \frac{\partial S_v}{\partial t} - \bar{\mu} + \frac{\dot{\delta}}{\hbar} + \sum_{j,k=x,z} \left(\dot{a}_j x_j + \dot{b}_{jk} x_j x_k \right) \right] \\ &= \rho - \frac{1}{g} \left[\frac{\hbar^2}{2M} |\nabla S|^2 + \hbar \frac{\partial S_v}{\partial t} + \frac{\dot{\delta}}{\hbar} + \sum_{j,k=x,z} \left(\dot{a}_j x_j + \dot{b}_{jk} x_j x_k \right) \right], \end{aligned} \quad (61)$$

where it is apparent that the terms $\dot{a}_j x_j$ account for displacements of the center of the condensate, and the terms $\dot{b}_{jk} x_j x_k$ incorporate changes in the radii and reorientation of the axes. One should notice the parallelism of this procedure with the method introduced in

Ref. [46] to analyze the effect of modulations of the trap frequencies on the fundamental state of a BEC. In that method, it is the form of the density that is explicitly proposed since physically supported conjectures can be made on it, the phase being subsequently derived from the Euler-like hydrodynamic equation. In contrast, in the present case, as it is the vorticity the characteristic of the structure that is actually known, it is convenient to start the proposal by modeling the phase.

We proceed as before using Eq. (13) to build the Lagrangian function from the proposed ansatz, and, later on, to obtain the Euler-Lagrange equations for the set of variational parameters. In order to have a first global picture of the dynamics, we have worked with a linearized version of the set of coupled equations. Within this regime, all the integrals have been obtained analytically beyond logarithmic accuracy to include zero order terms. The main implications of the coupling of vortex and fluid coordinates are summarized in the following points, where, to simplify the discussion we will not refer to the modulation mode identified in the previous subsection.

i) The vortex precession can be tracked down in one of the emerging normal modes. For the considered experimental conditions, given that the inertia of the condensate is much larger than that of the SV structure, the mixing of the former precession mode with the intrinsic condensate modes, incorporated via the parameters $a_j(t)$ and $b_{jk}(t)$, is negligible. Indeed, the *new version* of the precession mode basically corresponds to the motion of the vortex relative to the condensate. In contrast, there is a non-negligible displacement of the mode frequency with respect to the formerly obtained Ω_p . That shift is specifically rooted in the coupling with the parameters $a_j(t)$. Since its magnitude corresponds to a contribution of zero order in the quotient R_x/ξ , it can be incorporated into the functional form of Ω_p by modifying the effective zero-order parameter, which will be denoted now $c_\gamma^{(3)}$. Accordingly, the expressions of the precession frequencies corresponding respectively to the bosonic and fermionic cases are written as

$$\Omega_{p,B} = \frac{3 \hbar \sqrt{k_x k_z}}{4 \bar{\mu} M} \ln \left(c_{\gamma=1}^{(3)} \frac{R_x}{\xi} \right), \quad (62)$$

$$\Omega_{p,F} = \frac{\hbar \sqrt{k_x k_z}}{\bar{\mu} M} \ln \left(c_{\gamma=2/3}^{(3)} \frac{R_x}{\xi} \right). \quad (63)$$

ii) Among the resulting normal modes, one can also identify the dipole and quadrupole modes of the condensate. The effect of the vortex on those modes has been studied in

previous work [47, 48]. In agreement with the results of those studies, we observe that the presence of the vortex affects the frequencies of the quadrupole modes but leaves practically unchanged the frequencies of the dipole modes. The implications of a stronger mixing of the vortex dynamics and the condensate motion were analyzed in [49], where the setup characteristics correspond to a reduction in the magnitude of the inertia of the condensate relative to that of the vortex.

The results of the two studied extensions of the approach configure a picture where, the corrections to the previously presented (primary) description have a perturbative character.

VI. APPLICATION TO THE EXPERIMENTS

In order to illustrate the applicability of the study to emulate the results of the two considered experiments, we have incorporated into our approach the two sets of force constants used in the practical setups. Additionally, as amplitudes comparable to the TF radii were reached in both experiments, we have considered a broad range of amplitudes for the vortex motion.

Figs. 2 and 3 depict our findings for the (fermionic) system studied in [21]. In both figures, the precession period of the SV is displayed as a function of the chemical potential $\bar{\mu}$. (The precession period is expressed in units of the period $T_z = 2\pi/\omega_z$.) Whereas the results of Fig. 2 correspond to a linear regime, i.e., they are applicable when the amplitude is sufficiently small for the approximation $1 - A_{xz}^2 = 1 - X_0^2 - Z_0^2 \simeq 1$ to be valid, Fig. 3 incorporates nonlinear effects associated to increasing values of the amplitude. Moreover, in order to illustrate how the predictions on the SV behavior change as the sequence of extensions of the basic approach is applied, partial results, corresponding to the different stages in our model, are presented in Fig. 2. Namely, the dotted line reflects our primary picture, where the period is given by Eq. (49), with the effective zero-order parameter taking the value $c_\gamma^{(0)} = 1$. This description already improves the results of early analyses through the inclusion of anisotropy effects. Actually, at this stage, the main characteristics of the experimental curves are approximately reproduced. Still, observable corrections are obtained through the inclusion of additional effects. The dashed line, which corresponds to the first extension of the basic model, i.e., to the use of an ansatz where the precise connection between phase and density is incorporated, reflects a non-negligible modification of the period. A larger

additional shift (continuous line) is observed when the second extension of the model is applied, i.e., when, in addition to the previous system components, the coupling with the collective modes of the condensate is taken into account. The values $c_{\gamma=1}^{(3)} = 1.262$ and $c_{\gamma=2/3}^{(3)} = 0.876$, derived in our theoretical framework, were used to operatively incorporate the contribution of zero-order terms at this level. In the two considered regimes of the fermionic fluid, i.e., in the BEC side and in the unitary regime, the agreement with the experimental results improves as the description is generalized. Even so, it is the inclusion of nonlinearity in our framework that constitutes the dominant correction to the primary picture. As shown in Fig. 3, as larger amplitudes are reached, the period significantly decreases approaching the experimental results presented in [21]. (Note that the open circles correspond to experimental results extracted from Fig. 3 of [21].) It is also evident that although the agreement is good in the whole range considered for the chemical potential, the stronger dispersion of the experimental results in the unitarity regime makes the comparison to be less conclusive in that region. Actually, the need of a more detailed modeling of the system in that range might be conjectured. Namely, a more precise approximation to the size of the vortex core can be pertinent. In the same line, one must take into account that the polytropic approximation to the equation of state of the fluid, although appropriate to account for some significant aspects of the dynamics, cannot be expected to give a complete description of the system.

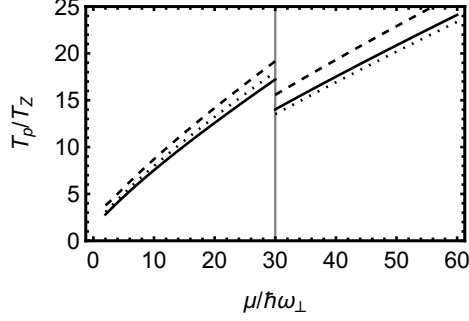


Figure 2: The precession period of the SV in a fermionic fluid as a function of the bulk chemical potential as given by the different approaches developed in the study. (The amplitudes are small enough to guarantee the applicability of a linear approximation.) The dotted line incorporates the results obtained through the basic approach. The dashed line corresponds to the first extension of the model. The continuous line represents the results of the complete (linear) description. The precession period is expressed in units of the period $T_z = 2\pi/\omega_z$ corresponding to the smallest of the trap frequencies, i.e., ω_z . Additionally, the chemical potential is written in units of $\hbar\omega_\perp \equiv \hbar\omega_x$. The figure illustrates the effect of the logarithmic factor $c_\gamma^{(i)}$ in each case. (The left and right regions respectively correspond to the BEC and unitary regimes.)

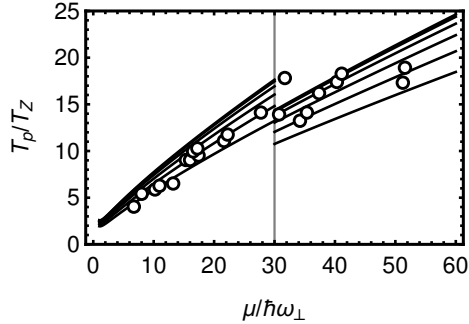


Figure 3: The precession period of the SV in a fermionic fluid as a function of the chemical potential for different amplitudes. The curves shift down as the amplitude A_{xz} takes larger values. ($A_{xz} = 0., 0.1, 0.2, 0.3, 0.4, 0.5$, from top to bottom.) The open circles correspond to experimental data extracted from Fig. 3 of [21]. (Same units as in Fig. 2.)

Additional arguments on the importance of including nonlinearity in the analyses can be extracted from Fig. 4, where the precession frequency corresponding to the setup of [26] is represented as a function of the amplitude. Actually, the reproduction of the experimental

results (see the spectral analysis presented in Fig. 6 of [26]) demands the introduction of non-linear corrections into the model. We recall that, in the early evaluation of the experiments of [26], the presence of SVs was merely conjectured since no confirmation through direct observation techniques was feasible. The agreement of our predictions with the experimental results supports the conjecture that the observed structures are actually SVs.

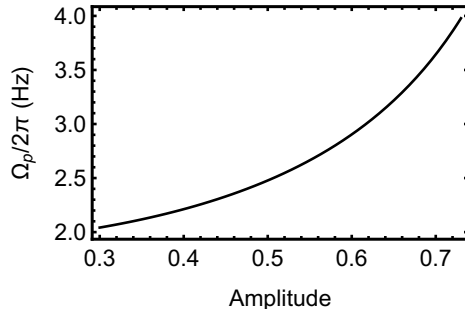


Figure 4: The precession frequency corresponding to the setup of [26] as a function of the relative amplitude A_{xz} .

VII. CONCLUDING REMARKS

Our study provides a theoretical framework for analyzing the dynamics of SVs in trapped superfluids which extends former approaches and allows clarifying recent experimental results. The unified approach applied to SVs in bosonic and fermionic superfluids has served to identify the common characteristics of the dynamics as simply rooted in the superfluid character of both systems. It has been shown that, in the regime where the hydrodynamic description is applicable, i.e., at scales much larger than the healing length, the only differential aspect of the fluid statistics is a numerical factor, dependent on the polytropic index, in the expression of the oscillation frequency. The general correspondence of our results with those of the experiments confirms the utility of the polytropic approximation to the equation of state of the fermionic fluid as an operative method to uncover basic aspects of the dynamics.

With respect to previous analyses of the considered experiments, the study contains specific advances in understanding the effect of the trap anisotropy, the relevance of nonlinearity to the SV precession, and the implications of the coupling with collective modes of the fluid. Indeed, the incorporation of a non-axisymmetric trap in the applied model has served to

trace the nontrivial dependence of the oscillation frequency on the anisotropy transversal to the vortical line. Moreover, nonlinearity has been found to be a central component of the dynamics emergent in the implemented setups. We have shown that the operatively defined inertial mass, apart from incorporating characteristics of the structure and trapping, is amplitude dependent. Additionally, the study has uncovered how the oscillation frequency is shifted by the coupling with collective modes of the fluid. The inclusion of those system components into our model implies a generalization of former descriptions which has led us to obtain precise values for the precession frequency, and, in turn, significantly improve the agreement with the experimental results. Our whole approach enhances the ground for the design of strategies of control.

Apart from accounting for features observed in the experiments, our analysis predicts the existence of fine details in the SV dynamics associated to potentially realizable experimental conditions. Indeed, the use of a variational ansatz where interrelated proposals for the phase and density are consistently incorporated has revealed the presence of a *fine structure* in the previously identified SV trajectories. The emergence of those fine details requires the implementation of specific initial conditions. Although technically demanding, their observation can be expected to be feasible given the significant advances achieved in the control of the considered systems. The modified ansatz has also served to give a more complete characterization of the vortex core. From our results, the validity of the basic modeling of the core is confirmed.

Some comments on potential extensions of the study are in order. No border effects have been incorporated into our approach: straight vortex lines have been considered. This simplification can be overcome through an appropriate modification of the functional form of the phase in the variational ansatz. The inclusion of dissipation effects, which can have practical implications on the controlled preparation of the systems and on the robustness of the predicted *fine structure* of the dynamics, is also pending. Moreover, we point out that the present study, focused on the dynamics subsequent to the SVs formation, does not complete the explanation of the experimental results. In fact, the characterization of the whole decay sequence, starting from PDS and ending with SVs is still required. In this line, the inclusion of additional structures in the decay process, like the intermediate solitonic form predicted in [11] and detected in [22], can be of great interest. Finally, it is worth stressing that alternative theoretical approaches which go beyond the hydrodynamic

description of the fermionic system are needed to characterize the vortex dynamics in the BCS regime.

Acknowledgments

One of us (JMGL) acknowledges the support of the Spanish Ministerio de Economía y Competitividad and the European Regional Development Fund (Grant No. PID2019-105225GB-I00).

-
- [1] J. Denschlag, J. E. Simsarian, D. L. Feder, C. W. Clark, L. A. Collins, J. Cubizolles, L. Deng, E. W. Hagley, K. Helmerson, W. P. Reinhardt, S. L. Rolston, B. I. Schneider, and W. D. Phillips, *Science* **287**, 97 (2000).
 - [2] B. P. Anderson, P. C. Haljan, C. A. Regal, D. L. Feder, L. A. Collins, C. W. Clark, and E. A. Cornell, *Phys. Rev. Lett.* **86**, 2926 (2001).
 - [3] D. J. Frantzeskakis, *J. Phys. A: Math. Theor.* **43**, 213001 (2010).
 - [4] A. Muryshv, G.V. Shlyapnikov, W. Ertmer, K. Sengstock, and M. Lewenstein, *Phys. Rev. Lett.* **89**, 110401 (2002).
 - [5] A. Weller, J. P. Ronzheimer, C. Gross, J. Esteve, M. K. Oberthaler, D. J. Frantzeskakis, G. Theocharis, and P. G. Kevrekidis, *Phys. Rev. Lett.* **101**, 130401 (2008).
 - [6] L. D. Carr, J. Brand, S. Burger, and A. Sanpera, *Phys. Rev. A* **63**, 051601(R) (2001).
 - [7] V.V. Konotop and L. Pitaevskii, *Phys. Rev. Lett.* **93**, 240403 (2004).
 - [8] N.S. Ginsberg, J. Brand, and L. V. Hau, *Phys. Rev. Lett.* **94**, 040403 (2005).
 - [9] S. Komineas and N. Papanicolaou, *Phys. Rev. A* **68**, 043617 (2003).
 - [10] A. A. Svidzinsky and A. L. Fetter, *Phys. Rev. Lett.* **84**, 5919 (2000).
 - [11] A. Muñoz Mateo and J. Brand, *New J. Phys.* **17**, 125013 (2015).
 - [12] A. Gaidoukov and J. R. Anglin, *Phys. Rev. A* **103**, 013319 (2021).
 - [13] D. L. Feder, M. S. Pindzola, L. A. Collins, B. I. Schneider, and C. W. Clark, *Phys. Rev. A* **62**, 053606 (2000).
 - [14] L.D. Carr, J. Brand, *Emergent Nonlinear Phenomena in Bose-Einstein Condensates: Theory and Experiment*, edited by P.G. Kevrekidis, D.J. Frantzeskakis, R. Carretero-Gonzalez

- (Springer, Heidelberg, 2007).
- [15] J. Brand and W.P. Reinhardt, Phys. Rev. A **65**, 043612 (2002).
 - [16] A. Munoz Mateo and J. Brand, Phys. Rev. Lett. **113**, 255302 (2014).
 - [17] I. Shomroni, E. Lahoud, S. Levy, and J. Steinhauer, Nat. Phys. **5**, 193 (2009).
 - [18] S. Donadello, S. Serafini, M. Tylutki, L. P. Pitaevskii, F. Dalfovo, G. Lamporesi, and G. Ferrari, Phys. Rev. Lett. **113**, 065302 (2014).
 - [19] A. Cetoli, J. Brand, R. G. Scott, F. Dalfovo, and L. P. Pitaevskii, Phys. Rev. A **88**, 043639 (2013).
 - [20] S. Giorgini, L. P. Pitaevskii, and S. Stringari, Rev. Mod. Phys. **80**, 1215 (2008).
 - [21] M. J. H. Ku, W. Ji, B. Mukherjee, E. Guardado-Sanchez, L. W. Cheuk, T. Yefsah, and M. W. Zwierlein, Phys. Rev. Lett. **113**, 065301 (2014).
 - [22] M. J. H. Ku, B. Mukherjee, T. Yefsah, and M. W. Zwierlein, Phys. Rev. Lett. **116**, 045304 (2016).
 - [23] M. J. H. Ku, A. T. Sommer, L. W. Cheuk, and M. W. Zwierlein, Science **335**, 563 (2012).
 - [24] M. Antezza, F. Dalfovo, L.P. Pitaevskii, and S. Stringari, Phys. Rev. A **76**, 043610 (2007).
 - [25] G. Lamporesi, S. Donadello, S. Serafini, F. Dalfovo, and G. Ferrari, Nature Phys. **9**, 656 (2013).
 - [26] A. R. Fritsch, Mingwu Lu, G. H. Reid, A. M. Pineiro, and I. B. Spielman, Phys. Rev. A **101**, 053629 (2020).
 - [27] S. Serafini, M. Barbiero, M. Debortoli, S. Donadello, F. Larcher, F. Dalfovo, G. Lamporesi, and G. Ferrari, Phys. Rev. Lett. **115**, 170402 (2015).
 - [28] M. Tylutki, S. Donadello, S. Serafini, L.P. Pitaevskii, F. Dalfovo, G. Lamporesi, and G. Ferrari, Eur. Phys. J. Special Topics **224**, 577–583 (2015).
 - [29] A. L. Fetter and J.-k. Kim, J. Low Temp. Phys. **125**, 239 (2001).
 - [30] L. Pitaevskii and S. Stringari, *Bose-Einstein Condensation* (Oxford University Press, Oxford, U.K., 2003); C. J. Pethick and H. Smith, *Bose-Einstein Condensation in Dilute Gases* (Cambridge University Press, Cambridge, U.K., 2008).
 - [31] W. Ketterle and M. Zwierlein, Riv. Nuovo Cimento Soc. Ital. Fis. **31**, 247 (2008).
 - [32] *The BCS-BEC Crossover and the Unitary Fermi Gas*, edited by W. Zwerger (Springer, New York, 2011), Vol. 836.
 - [33] M. Cozzini and S. Stringari, Phys. Rev. Lett. **91**, 070401 (2003).
 - [34] W. Wen, C. Zhao, and X. Ma, Phys. Rev. A **88**, 063621 (2013).

- [35] N. Manini and L. Salasnich, Phys. Rev. A **71**, 033625 (2005).
- [36] V.M. Perez-García, H. Michinel, J. I. Cirac, M. Lewenstein, and P. Zoller, Phys. Rev. Lett. **77**, 5320, (1996).
- [37] L. P. Pitaevskii, arXiv:1311.4693.
- [38] A. Bulgac, Michael McNeil Forbes, M. M. Kelley, K. J. Roche, and G. Wlazłowski, Phys. Rev. Lett. **112**, 025301 (2014).
- [39] M. D. Reichl and E. J. Mueller, Phys. Rev. A **88**, 053626 (2013).
- [40] E. Lundh and P. Ao, Phys. Rev. A **61**, 063612 (2000).
- [41] P. O. Fedichev, A. E. Muryshev, and G. V. Shlyapnikov, Phys. Rev. A **60**, 3220 (1999).
- [42] P. O. Fedichev and G. V. Shlyapnikov, Phys. Rev. A **60**, R1779 (1999).
- [43] S. Burger, K. Bongs, S. Dettmer, W. Ertmer, K. Sengstock, A. Sanpera, G. V. Shlyapnikov, and M. Lewenstein, Phys. Rev. Lett. **83**, 5198 (1999).
- [44] H. M. Hurst, D. K. Efimkin, I. B. Spielman, and V. Galitski, Phys. Rev. A **95**, 053604 (2017).
- [45] R. G. Scott, F. Dalfovo, L. P. Pitaevskii, and S. Stringari, Phys. Rev. Lett. **106**, 185301 (2011).
- [46] Y. Castin and R. Dum, Phys. Rev. Lett. **77**, 5315 (1996).
- [47] A. A. Svidzinsky and A.L. Fetter, Phys. Rev. A **58**, 3168 (1998).
- [48] F. Zambelli and S. Stringari, Phys. Rev. Lett. **81**, 1754 (1998).
- [49] M. Linn and A. L. Fetter, Phys. Rev. A **61**, 063603 (2000).